RESEARCH ARTICLE | NOVEMBER 08 2018

Particles-based thermal energy storage systems for concentrated solar power

Miguel A. Reyes-Belmonte; Elena Díaz; Manuel Romero; José González-Aguilar

AIP Conf. Proc. 2033, 210013 (2018)
https://doi.org/10.1063/1.5067215

Particles-based Thermal Energy Storage Systems for Concentrated Solar Power

Miguel A. Reyes-Belmonte[1], Elena Díaz[1], Manuel Romero[1] and José González-Aguilar[1,a]

[1]*IMDEA Energy Institute, Avda. Ramón de la Sagra 3, 28935, Móstoles, Madrid (Spain)*

[a)] Corresponding author: jose.gonzalez@imdea.org

Abstract. In this paper, particles-based thermal energy storage (TES) system for concentrated solar power (CSP) is presented and applied to different CSP plant-layout scenarios. The key-component of this system is the fluidized-bed heat exchanger (DPS-HX) that is used for coupling particles-based storage system to the solar loop and to the power block. Mathematical model is used for the design and thermal performance analysis of the heat exchanger coupled to subcritical and supercritical Rankine steam cycles for small and commercial plant sizes. Among the benefits of particles-based thermal energy storage it can be pointed out no temperature restrictions with no freezing nor temperature degradation, ease of handling and no toxicity. It has been found that particles heat exchanger operates at high efficiency (from 91% to 99% for most of cases) and that power consumption for fluidization purposes are negligible compared to thermal power transferred to the work transfer fluid. For large power plant size, it is preferred distributing particles among different heat exchangers connected in parallel instead of passing whole particles and work transfer fluid through just one heat exchanger component.

INTRODUCTION

Concentrated solar power (CSP) is one of the most promising technologies for electricity production in a scenario of high penetration of renewable energy sources. This is due to the flexible electricity dispatch when it is coupled to thermal energy storage (TES) systems. Despite the environmental benefits and abundant solar resource, a step further is needed for CSP technology deployment mainly due to the extensive land utilization and limited operative temperatures which are translated into still high costs for electricity production. In order to improve CSP competitiveness, moving towards more efficient power cycles, which is thermodynamically related to higher operating temperatures or the use of new working fluids, is seen as the next step on CSP research. In that frame, a new concept based on the utilization of dense particles suspension (DPS) as heat transfer fluid (HTF) and TES for CSP plants introduces an extraordinary level of freedom for highly efficient power plant design. The use of DPS as HTF is not restricting solar plant operative working temperatures [1] since neither freezing nor degradation of particles occurs, in addition, it is cheap[2] and abundant material, with no toxic consequences.

Recently a growing interest on the use of particles for solar receivers and CSP applications [2–4] has appeared based on the abovementioned benefits that will contribute on the deployment of a new generation of CSP plants. This interest has been reinforced by several public funded research projects for investigating on particles-based solar power plants [5–7]. One of the key features about using particles for CSP applications is related to the TES system as no temperature constraints appear and its ease for handling and transportation. Due to those reasons, several researchers are proposing the use of particles-based TES systems for CSP plants [8–11]. The novelty of this work compared to previous research in this field is based on the detailed design proposal and thermal characterization of fluidized-bed heat exchangers (DPS-HX) connecting particles-based TES storage to subcritical and supercritical water-steam Rankine cycles for both small and large sizes. HX effectiveness, efficiency, temperature profiles and sizes are investigated for each case as well as sizing recommendations are provided for scaling-up scenario.

SolarPACES 2017
AIP Conf. Proc. 2033, 210013-1–210013-8; https://doi.org/10.1063/1.5067215
Published by AIP Publishing. 978-0-7354-1757-1/$30.00

Nomenclature			
CSP	Concentrated Solar Power	g	Fluidization gas (air)
DPS	Dense Particle Suspension	Q	Thermal power
FB	Fluidized Bed	s	Supercritical conditions (or solid particles)
HTF	Heat Transfer Fluid	T	Temperature
HX	Heat Exchanger	γ_T	Temperature-based efficiency
TES	Thermal Energy Storage	γ	Thermal efficiency
WF	Work Transfer Fluid		

SOLAR PLANT DESCRIPTION

TES concept presented in this work allows decoupling the solar loop and the power block by introducing intermediate particles-based TES system. As it can be observed on FIGURE 1, flexible CSP design can be achieved since any HTF can be used for the solar loop while any work transfer fluid (WTF) can run the power block due to the intermediate particles-based TES system. Furthermore, neither temperature restrictions nor phase change are limiting factors for this application and therefore higher efficiency can be pursued for the power block. This concept allows introducing very efficient power blocks (combined cycle, supercritical steam or sCO_2) for CSP applications[12,13] as well as moving towards cheaper HTF for solar receivers as for example air. In addition, extra level of freedom can be achieved by decoupling the solar loop and power conversion which simplifies the operation of the power cycle while mitigating the effect of transient weather conditions. Particles-based TES provides cheap energy storage solution due to the inexpensive price of bulk material (sand, silicon carbide or olivine), its ease for silo storage and transportation (screw, bend conveyors or elevator buckets). One of the key elements of particles-based TES concept proposal is the heat exchanger design that is connecting particles storage system to whether the solar loop or the power block.

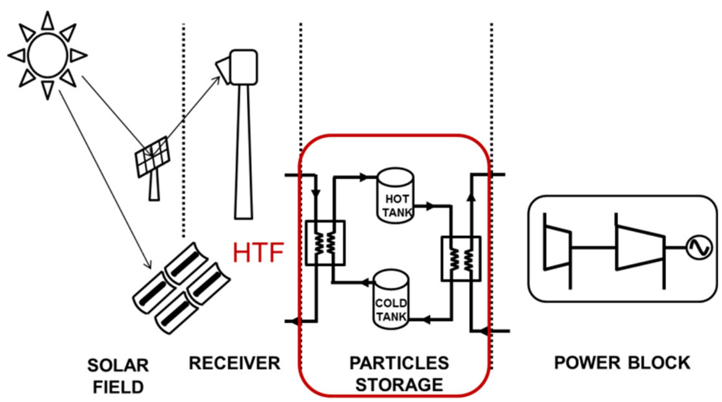

FIGURE 1. Power plant layout by introducing particles-based TES intermediate system

HEAT EXCHANGER MODEL DESCRIPTION

Heat exchanger model is based on fluidized bed technology applied to tubes and shell configuration [14] where HTF (or WTF) passes along the bundle of tubes while cold (or hot) particles are fluidized using injected air stream from below the container [8]. Detailed working principle and operation scheme can be found on previous works[14]. Fluidized particles in contact with tubes bundles absorb or transfer the sensible heat according to complex heat transfer mechanism depending on the air velocity, particles size and volume proportion of air and particles suspension, heat transfer fluid velocities or heat exchanger dimensions. Solving methodology [15] is based on physical and empirical heat transfer correlations applied to horizontal tubes immersed on dense particle suspension. Heat transfer correlations can be adapted to account for any HTF or WTF inside the tubes, in this work subcritical and supercritical steam have been considered due to the power block. Applying the solving methodology, heat exchanger sizing (number of tubes, number of stages, length, and diameters), fluidization conditions (particles mass flow, fluidization air mass flow and power consumption) and thermal performance (efficiency and temperature profiles) are determined given boundary conditions (steam target temperature and thermal power to exchange).

RESULTS ANALYSIS

In this section, thermal performance and geometrical design for DPS-HX needed connecting particles-based TES system to steam Rankine cycles are analyzed. Two power block scenarios (subcritical and supercritical steam Rankine cycles) and two different power plant capacities (small and large power) have been considered (**TABLE 1**).

TABLE 1. Boundary conditions for DPS-HX

Cycle	Supercritical		Subcritical	Supercritical		Subcritical
Steam target temperature	~ 585 ºC	~ 650 ºC	~ 585 ºC	~ 585 ºC	~ 650 ºC	~ 585 ºC
Thermal power exchanged to the power cycle	~ 30 MW			~ 300 MW		
Water/steam inlet temperature to DPS-HX	233 ºC					
Particles hot temperature	~720 ºC					
Particles cold temperature	~300 ºC					

DPS-HX Thermal Performance

In this section, thermal performance of the different DPS-HX used for coupling particles-based TES system to the selected power blocks is analyzed. Temperature profiles, thermal efficiency and heat losses of heat exchangers are represented for each stage. Due to the high number of DPS-HX model parameters, multiple solutions for its geometrical design can be found that are satisfying boundary conditions from **TABLE 1**.

Small Power Scale

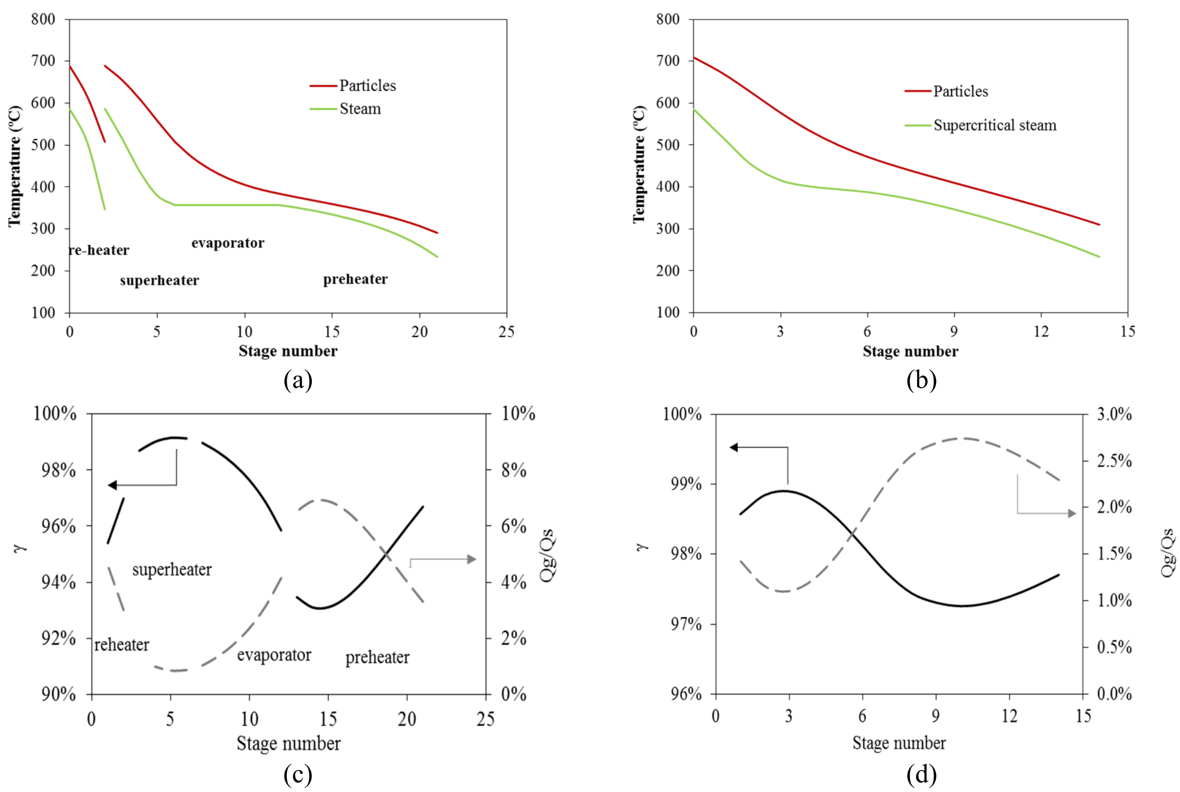

FIGURE 2. DPS-HX performance for small power case (30 MWth). (a) Temperature profile of DPS-HX coupled to subcritical steam Rankine cycle. (b) Temperature profile of DPS-HX coupled to supercritical steam Rankine cycle. (c) Thermal performance of DPS-HX coupled to subcritical steam Rankine cycle. (d) Thermal performance of DPS-HX coupled to supercritical steam Rankine cycle.

DPS-HX thermal performance on **FIGURE 2** represents one of the multiple solutions found for particles heat exchanger design able to reproduce boundary conditions from **TABLE 1** for the smallest power block capacity (30 MW) and same turbine inlet temperature (580 ºC). This solution was preferred among others due to its more compact design (less number of stages), smallest temperature drop between hot particles and steam that allows better utilization of energy and the lowest thermal energy losses due to the fluidization air. These losses are defined as the ratio between the heat power removed by the fluidization air (Q_g) and the total thermal power stored by particles (Q_{DPS}) as represented by eq. (1).

$$1-\gamma=\frac{Q_g}{Q_{DPS}} \tag{1}$$

Where γ is the thermal efficiency of the heat exchanger and has been defined in this work as the ratio between transferred thermal power to the steam (Q_{WF}) and the stored energy by particles (Q_{DPS}) shown by eq. (2).

$$\gamma=\frac{Q_{WF}}{Q_{DPS}} \tag{2}$$

Series in dark color line are showing temperature evolution of particles while series in light color are showing the work transfer fluid temperature evolution (the steam that will be used for running the power cycle). Pictures on the left are showing subcritical working conditions. As it can be observed from graphs (c) and (d) of **FIGURE 2**, thermal efficiency of design DPS-HX changes from 93% to 99% depending on the stage number for subcritical steam case, while it fluctuates less around 97% and 99% for supercritical steam. This indicates that thermal energy that is taken by the fluidization air and cannot be recovered for working fluid heating is below 5% for most of cases. In both Rankine cycles, typical turbine inlet steam conditions have been considered (580 ºC at 180 bar for subcritical case and 650 ºC at 285 bar for the supercritical cycle).

Large Power Scale

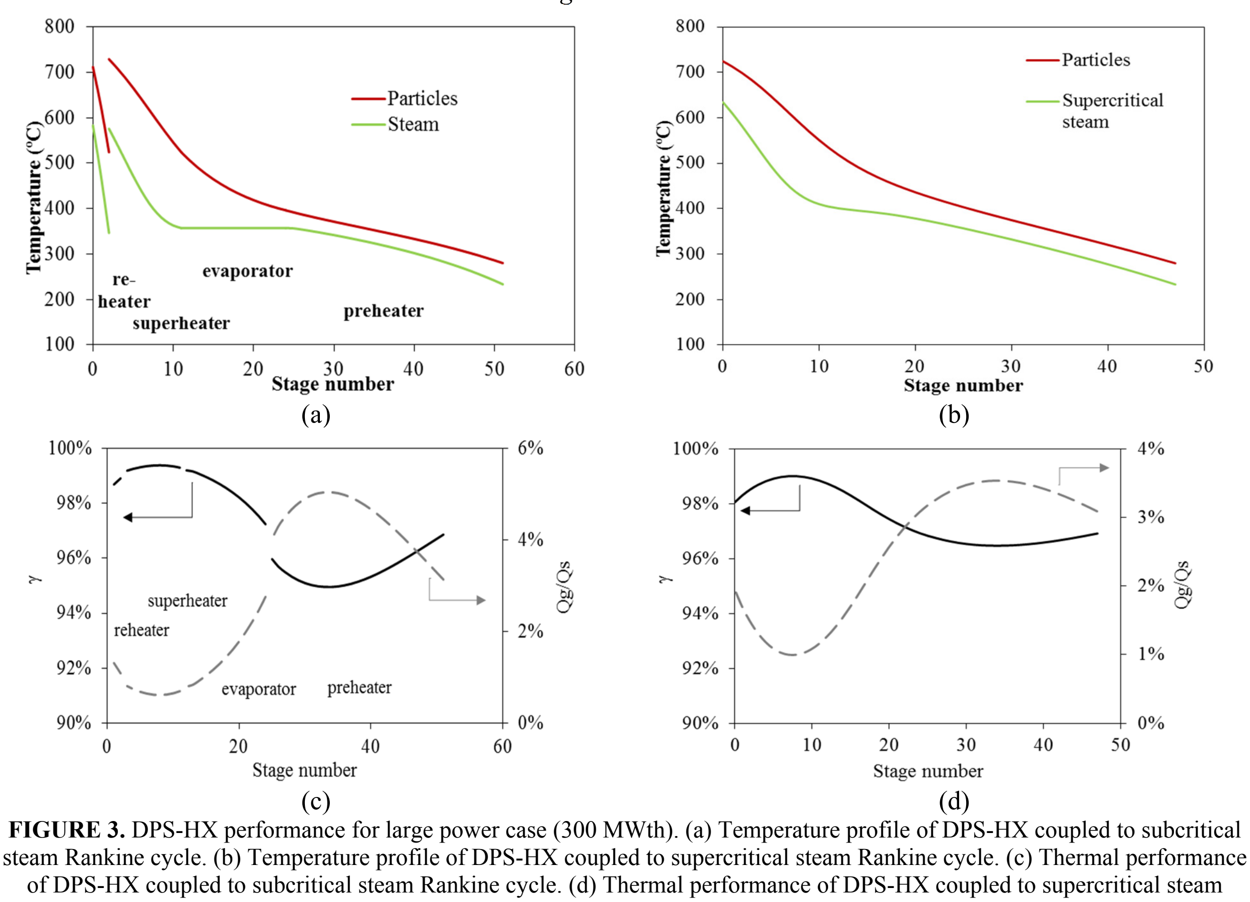

FIGURE 3. DPS-HX performance for large power case (300 MWth). (a) Temperature profile of DPS-HX coupled to subcritical steam Rankine cycle. (b) Temperature profile of DPS-HX coupled to supercritical steam Rankine cycle. (c) Thermal performance of DPS-HX coupled to subcritical steam Rankine cycle. (d) Thermal performance of DPS-HX coupled to supercritical steam Rankine cycle.

FIGURE 3 represents the thermal performance of DPS-HX connecting particles TES system to large power block capacity (300 MW) mounting reheated subcritical steam and supercritical steam Rankine cycles. As it can be observed comparing graphs (a) and (b), temperature drop between hot particles and steam is reduced for the supercritical case due to there is no pinch point restriction associated to water/steam phase change process, this is leading to a better utilization of thermal energy and a more compact design as it will be discussed at Results and Discussion section.

RESULTS AND DISCUSSION

As it can be deduced from **FIGURE 2** and **FIGURE 3**, increasing the thermal power by one order of magnitude (30 MW to 300 MW) was not translated to an increase of 10 times the number of required DPS-HX stages or the number of tubes (**TABLE 2** and **TABLE 3**). Nevertheless, internal diameter of heat exchanger tubes needed to be enlarged (from 25.4 mm to 45 mm) in order to keep water/steam velocity and pressure drop inside tubes below typical values which was translated into higher surface exchange areas. As it can be observed on **TABLE 2**, three different cases were analyzed for each power size. One subcritical Rankine cycle was studied at 580 ºC steam temperature while two different scenarios were considered for the supercritical case. One cycle keeping the same temperature (580 ºC) for comparison purposes while the other supercritical cycle was at higher temperature (650 ºC) for maximizing potential of supercritical steam. As it is observed, temperature-based efficiency of the heat exchanger considerably improves for the high temperature supercritical cycle, since it is easier finding a solution with small temperature drop between hot particles and steam as pinch temperature is not limiting heat exchanger design. DPS-HX temperature-based efficiency is defined according to eq. (3). That represents the existing temperature rise on the WF compared to the maximum temperature rise available from hot particles.

$$\gamma_T = \frac{T_{WF,out} - T_{WF,in}}{T_{DPS,out} - T_{WF,in}} \tag{3}$$

TABLE 2. Thermal performance of DPS-HX connecting particles-based storage to different steam Rankine cycles.

Scale	**30 MW**			**300 MW**		
Cycle	**Supercritical**	**Supercritical (higher T)**	**subcritical**	**Supercritical**	**Supercritical (high T)**	**subcritical**
Thermal power exchanged to the power cycle	28 MW	27 MW	29 MW	292 MW	289 MW	286 MW
Particles flow	65 kg/s	60 kg/s	66 kg/s	630 kg/s	600 kg/s	610 kg/s
Water/Steam flow	11 kg/s	10 kg/s	8 kg/s	120 kg/s	110 kg/s	90 kg/s
Total number of stages	14	14	23	46	48	51
Hot tank particles temperature	709 ºC	730 ºC	700 ºC	718 ºC	735 ºC	729 ºC
Cold tank particles temperature	310 ºC	310 ºC	291 ºC	280 ºC	280 ºC	280 ºC
Steam final temperature	585 ºC	650 ºC	580 ºC	590 ºC	657 ºC	580 ºC
Steam pressure	285 bar	285 bar	180 bar	285 bar	285 bar	180 bar
Water/Steam initial temperature	233 ºC	233 ºC	233 ºC	233 ºC	233 ºC	233 ºC
Fluidization power consumption	0.02 MW	0.02 MW	0.03 MW	0.24 MW	0.25 MW	0.24 MW
Global heat exchanger efficiency (γ)	98.2%	98.2%	97.9%	98.1%	98.0%	98.2%
Temperature-based heat exchanger efficiency (γ_T)	73.9%	83.9%	74.3%	73.6%	84.5%	70.0%

In all studied cases, inlet water temperature to the DPS-HX was a boundary condition determined from energy recuperation schemes of the Rankine cycle whose different turbine steam extractions allowed water preheating after power block economizer. As it can be observed from **TABLE 2**, particles-based TES system allows extending the temperature range of the storage system (from 280 ºC to 730 ºC) compared to commercial current solution using molten salts (from 290 ºC to 565 ºC). As it can be deduced from **TABLE 2**, hot particles need to be heated above 700 ºC for coupling designed DPS-HX to the proposed power cycles in **TABLE 1**. In other words, hot particles used for TES system should be from 50 ºC to 120 ºC above the target temperature of the WF (steam) depending on the selected power cycle. This scenario could be achieved by using particles receiver approach[1] where particles are used for both solar loop and TES loop. Those conditions could be also achieved in case of using particles-based TES system as an intermediate loop (**FIGURE 1**) for high temperature thermal energy storage such as air receivers or integrated solar combined cycles (ISCC). Apart from temperature-based efficiency of the DPS-HX, **TABLE 2** is also providing two other useful parameters for DPS-HX thermal characterization. On the one hand it is provided, global heat exchanger efficiency that was mentioned above in equation (2) which is related to the thermal power removed by the fluidization air. Those losses were around 2% - 4% of the total transferred power. On the other hand, it is provided the power consumption needed for fluidizing particles inside the heat exchanger, this power represents compression work required for air injection below container of DPS-HX. As it can be observed, air compression power is negligible compared to the transferred thermal power (less than 0.1 %).

Geometry Design

TABLE 3 presents geometrical parameters of solution found for DPS-HX for different power blocks (subcritical and supercritical steam Rankine) and plant capacity (30 MW and 300 MW). For the case of subcritical Rankine cycle, geometrical parameters have been provided for the different components of the DPS-HX (preheater, evaporator, superheater and reheater). As it was mentioned above, multiple solutions will exist for the geometrical design of the DPS-HX provided the same boundary conditions. Different combinations of number of tubes, bundles, stages, tubes length and diameters will provide same target steam temperature but following different temperature profiles. Option presented on **TABLE 3** was a compromise solution giving the lower temperature drop between hot particles and steam (what improved energy utilization) with a reasonable size of the heat exchanger. As it can be observed for the smaller power case (30 MW), lower heat exchanger size was needed for the supercritical Rankine cycle compared to the subcritical cycle. This was due to better energy utilization since no pinch point restriction. As it can be observed, tubes diameter are enlarged for large power case. Same number of DPS-HX tubes was kept for both small and large power cases, and even same tubes length for subcritical DPS-HX independently of its power.

TABLE 3. Geometrical design of the DPS-HX connecting particles-based storage to different steam Rankine cycles.

Thermal power (MW)	Power Block		Tubes per bundle	Bundle per stage	Tube length (m)	Tubes diam. (mm)	Stage total length (m)	Stage exch. area (m^2)	Stages	Total exch. area (m^2)
30	Supercritical		53	3	4.4	25.4	700	55.8	14	782
	Supercritical (higher T)		53	3	4.4	25.4	700	55.8	14	782
	Subcritical	Preheating	53	3	4.4	25.4	700	55.8	9	502
		Evaporator	50	3	4.2	25.4	630	50.3	6	302
		Superheating	42	1	3.5	25.4	147	11.7	4	47
		Reheating	90	1	7.4	25.4	666	53.1	2	106
300	Supercritical		53	3	7.8	45.0	1235	174.7	46	8034
	Supercritical (higher T)		53	3	7.8	45.0	1235	174.7	48	8383
	Subcritical	Preheating	53	3	4.4	45.0	700	98.9	25	2473
		Evaporator	50	3	4.2	45.0	630	89.1	13	1158
		Superheating	42	1	3.5	45.0	147	20.8	9	187
		Reheating	90	1	7.4	45.0	666	94.2	2	188

Scaling-up Proposal

As it was observed on **TABLE 3**, large contact areas were required for DPS-HX in order to compensate the low energy density of particles suspension. In order to avoid very large designs of the heat exchanger with many stages connected in series or using very large tubes, scaling-up solution was proposed. According to this proposal (**TABLE 4**), multiple DPS-HX bodies could be connected in parallel. In this case, each line will work under same temperature boundary conditions and inlet and outlet temperatures while particles and water/steam mass flow will be divided evenly among the number of lines. This approach will reduce water/steam pressure losses inside the heat exchanger due to the lower mass flow, shorter tubes and lower number of stages connected in series as it can be observed on **TABLE 4**. The case of using 10 modules in parallel was explored and as it can be observed, the total exchange area of DPS-HX could be reduced up to 5% due to smaller tubes diameters and shorter length. In addition, parallel configuration allows increasing power plant capacity in a modular way by adding extra lines since DPS-HX design would remain the one from the small power plant capacity that was shown in **TABLE 3.**

TABLE 4. DPS-HX scaling-up modular design proposal

	Thermal power (MW)	**300**			
	Power Block	**Supercritical (585 ºC)**		**Supercritical (650 ºC)**	
Per line	Number of lines	1	10	1	10
	Number of tubes/bundle	53	53	53	53
	Number of bundles/stage	3	3	3	3
	Tube length (m)	7.8	4.4	7.8	4.4
	Tubes diameter (mm)	45.0	25.4	45.0	25.4
	Stage total length (m)	1235	700	1235	700
	Stage exchange area (m^2)	175	56	175	56
	Number of stages	46	14	48	14
	Total exchange area (m^2)	8034	782	8383	782
	Heat exchanger steam pressure drop (bar)	10.2	1.9	8.6	1.8
Total	Number of stages	46	140	48	140
	Exchange area (m^2)	8034	7816	8383	7816
	Pumping losses power (MW)	4.6	0.2	5.6	0.2

CONCLUSIONS

In this paper it has been presented the design proposal and thermal performance evaluation of particles heat exchanger for connecting particles-based thermal energy storage system to different power blocks in concentrated solar power applications. In particular, six different scenarios have been analyzed for two different power cycles (subcritical and supercritical steam Rankine cycles), two different power plant capacities (small and large) and two different temperature levels. As it was discussed along the paper, efficient design of DPS-HX can be found for transferring thermal energy from hot particles to water/steam WF with a global efficiency above 95% for most of the studied cases while energy required for air fluidization (compression work) was below 0.1%. As it was discussed, several HX arrangements could be found for satisfying modelling boundary conditions, nevertheless preferred option providing compact design and small temperature drop between hot particles and steam was chosen for better energy utilization. In case of large power plant capacity scenario, it was found that DPS-HX contact area should be largely increased for compensating low energy density of particles. As a way for reducing the surface area, it was proposed a different configuration splitting the total DPS-HX into different modules in parallel what led to smaller contact area.

ACKNOWLEDGMENTS

The research leading to these results has received funding from EU FP7/2013-2017 under grant agreement n° 609837 (FP7 IRP STAGE-STE) and from the European Union's Horizon 2020 research and innovation program under grant agreement No 727762, Next-CSP project. Authors would like to thank "Comunidad de Madrid" support to the ALCCONES project (S2013/MAE-2985) through R&D activities Program between research groups 2103 and "Ministerio de Economía y Competitividad" support through Research Challenges project ARROPAR-CEX (ENE2015-71254-C3-1-R). E. Díaz is grateful to Spanish Ministry of Education, Culture and Sport by funding through internship FPU (FPU16/00217).

REFERENCES

1. Benoit, H., Pérez López, I., Gauthier, D., Sans, J.-L. & Flamant, G. On-sun demonstration of a 750°C heat transfer fluid for concentrating solar systems: Dense particle suspension in tube. *Solar Energy* **118,** 622–633 (2015).
2. Spelling, J., Gallo, A., Romero, M. & González-Aguilar, J. A High-efficiency Solar Thermal Power Plant using a Dense Particle Suspension as the Heat Transfer Fluid. *Energy Procedia* **69,** 1160–1170 (2015).
3. Ma, Z., Glatzmaier, G. & Mehos, M. Fluidized Bed Technology for Concentrating Solar Power With Thermal Energy Storage. *Journal of Solar Energy Engineering* **136,** 31014 (2014).
4. Ho, C. K. A review of high-temperature particle receivers for concentrating solar power. *Applied Thermal Engineering* **109,** 958–969 (2016).
5. CSP2: Concentrated Solar Power in Particles. *European Comission* (2013). at <http://www.csp2-project.eu/>
6. NEXT-CSP: High Temperature concentrated solar thermal power plant with particle receiver and direct thermal storage. *European Comission* (2016). at <http://next-csp.eu/>
7. Sunshot. *High-Temperature Falling-Particle Receiver*. *U.S. Department of Energy* (2012). at <www.solar.energy.gov/sunshot/csp_sunshotrnd_snl.html>
8. Schwaiger, K. *et al.* SandTES - An active thermal energy storage system based on the fluidization of powders. *Energy Procedia* **49,** 983–992 (2013).
9. Steiner, P., Schwaiger, K. & Walter, H. Active Fluidized Bed Technology Used for Thermal Energy Storage. in *Proceedings of the ASME 2016 10th International Conference on Energy Sustainability* (ed. ASME) 1–10 (2016).
10. Ma, Z., Glatzmaier, G. C. & Mehos, M. Development of Solid Particle Thermal Energy Storage for Concentrating Solar Power Plants that Use Fluidized Bed Technology. *Energy Procedia* **49,** 898–907 (2014).
11. Sakadjian, B. *et al.* Fluidized-bed technology enabling the integration of high temperature solar receiver CSP systems with steam and advanced power cycles. *Energy Procedia* **69,** 1404–1411 (2015).
12. Reyes-Belmonte, M. A. *et al.* Heat exchanger modelling in central receiver solar power plant using dense particle suspension. in *AIP Conference Proceedings* **1850,** 30042 (AIP Publishing LLC , 2017).
13. Reyes-Belmonte, M. A., Sebastián, A., Romero, M. & González-Aguilar, J. Optimization of a recompression supercritical carbon dioxide cycle for an innovative central receiver solar power plant. *Energy* **112,** 17–27 (2016).
14. Gomez-Garcia, F., Gauthier, D. & Flamant, G. Design and performance of a multistage fluidised bed heat exchanger for particle-receiver solar power plants with storage. *Applied Energy* **190,** 510–523 (2017).
15. Reyes-Belmonte, M. A., Sebastián, A., González-Aguilar, J. & Romero, M. Performance comparison of different thermodynamic cycles for an innovative central receiver solar power plant. in *AIP Conference Proceedings* **1850,** 160024 (AIP Publishing LLC , 2017).